Carpathian Journal of Earth and Environmental Sciences, February 2014, Vol. 9, No. 1, p. 57 - 68

ALLANITE AND MONAZITE OCCURRENCES IN VARISCAN GRANITOIDS OF TISZA MEGA-UNIT (SOUTH HUNGARY)

György BUDA[1], Géza NAGY[2] & Elemér PÁL-MOLNÁR[3,4]

[1]Department of Mineralogy, Eötvös Loránd University, H-1117 Budapest, Pázmány P. Street 1/C, Hungary
e-mail: buda@ludens.elte.hu
[2]Institute for Geological and Geochemical Research, Research Centre for Astronomy and Earth Sciences, Hungarian Academy of Sciences, H-1112 Budapest, Budaörsi Street 45, Hungary; e-mail: gnagy@geochem.hu
[3]Department of Mineralogy, Geochemistry and Petrology, University of Szeged, H-6701 Szeged, P.O. Box 651, Hungary
[4]MTA-ELTE Volcanology Research Group, H-1117 Budapest, Pázmány P. Street 1/C, Hungary
e-mai: palm@geo.u-szeged.hu

Abstract: Two main Variscan granitoid plutons are in the Tisza Mega-Unit of south Hungary. The older one (~340 Ma) belongs to the magnesio-potassic, met- to peraluminous calc-alkaline monzonitic series with abundant mafic enclaves in Mórágy Subunit. In the whole intrusive body, allanite-(Ce) crystallized along with apatite and titanite as accessory minerals due to high Ca activity. The high concentration of Ca and low Al in the melts favoured the crystallization of allanite. The chondrite-normalized REE pattern of the host rock is controlled by the REE-rich allanite-(Ce). High oxidation of the unaltered allanite indicates crystallization under high oxygen fugacities from high-temperature I-type granitoid magma. Allanite crystallization was continuous over the entire magma solidification, as revealed by the abundant presence of rock-forming mineral inclusions. Volatile-rich post-magmatic hydrothermal solutions altered the allanite-(Ce) in different ways depending on the pH of solutions. Alkali-rich solutions leached Si and Al, whereas acidic fluids dissolved and transported the REE, depositing them on the rims of crystals or in nearby cracks as a form of fluorcarbonates. Some zoned crystals preserved the original magmatic REE zonation after leaching of Al and Si. The younger plutons (300–325 Ma) occur in the southeast part of the Tisza Mega-Unit in the Battonya Subunit. They consist of peraluminous, monazite-rich, high Al, low Ca, two-mica and muscovite granodiorite-granite with mafic enclaves. The muscovite-rich granitoids are S-type and belong to the monazite-type calc-alkaline granodioritic series with some metaluminous amphibole-bearing enclaves.

Keywords: I-, S-type granitoids, allanite-(Ce), monazite-(Ce), REE distribution, alteration, Mórágy Subunit, Battonya Subunit, south Hungary

1. INTRODUCTION

In granitoid rocks the REE (rare earth elements), Zr, Hf, U, Th, Y, Ti, and P concentrations are controlled by accessory minerals such as allanite-(Ce), monazite-(Ce), xenotime-(Y), apatite, zircon, thorite, sphene, magnetite, and ilmenite. The REE distribution of the host rocks is governed mainly by allanite-(Ce), monazite-(Ce) (xenotime), apatite, zircon, and titanite. The granitoid melt, which originated from the melting of igneous rocks (I-type) at high temperature, contains low Al (metaluminous) and high Ca. High concentrations of Ca increase the stability field of allanite-(Ce) in melts (Johannes & Holtz, 1996) and therefore, in these rocks Ca-bearing REE-rich allanite-(Ce) is common (allanite-type granitoid) and REE-rich apatite is widespread. Varieties with amphibole contain REE-bearing titanite as well. Oxygen fugacity is high as a consequence of the higher temperature of the silicate melt, Fe is oxidized, and magnetite, Fe^{3+}-bearing allanite, and Mn-poor apatite are crystallized.

Granitoid melts derived by melting of sedimentary rocks (S-type) contain high Al (peraluminous) and low Ca. The melting temperature and oxygen fugacity are low, mostly Fe^{2+} and Mn^{2+} are present in biotite as well as in apatite, and ilmenite is crystallized (ilmenite-type

granitoid). Light Rare Earth Elements (LREE) bearing mineral is mainly monazite-(Ce) (monazite-type granitoid), and Heavy Rare Earth Elements (HREE) occurs in rare xenotime-(Y). Apatite is depleted in REE and enriched in Mn. According to Spicer et al., (2006), rounded crystal habits of apatite and monazite-(Ce) in this granite are sedimentary relics of the source rocks.

Allanite-(Ce) is present in rocks that contain high CaO (>2.0 wt %), but only monazite-(Ce) occurs in rocks that contain low CaO (<0.7%). Both allanite-(Ce) and monazite-(Ce) are present at intermediate CaO values (Lee & Bastron, 1967).

At higher values of D [Na+K+2Ca/Al*(Si+Al)>1.1] and temperatures, the H_2O dissolves monacite, and allanite-(Ce) forms, according to experiments by Montel (1993).

I- and S-type granitoids occur in the Tisza Mega-Unit (Hungary). The purpose of this study is to determine the geochemical characteristics of REE-bearing accessory minerals in these rocks.

2. GEOLOGICAL SETTING

The present geological and tectonic setting of the Carpathian or Pannonian Basin resulted from multi-step evolution of geological structures. The complexity is due to the tectonic position of the territory. It is situated in a collision zone of the European and African continental plates. The history began with spreading, followed by a series of collisions. During the Alpine orogeny, the drifting and welding of the individual fragments were accompanied by folding and nappe formation. At the end of the Miocene, the attenuation of the crust (upward bulging of the mantle) resulted in the development of a large basin that determines the present structural setting of the area.

The greatest part of the pre-Neogene basement of the Pannonian Basin is composed of two megatectonic units divided by the so-called Mid-Hungarian Lineament in the NE–SW direction (between Zagreb and Zemplen). North from the lineament, the Alp-Carpathian-Pannonian (ALCAPA) Mega-Unit occurs, whose southern part is the Pelso Composite Unit, while the Tisza Mega-Unit (TMU) is situated in the south (Fig. 1/A; Pál-Molnár et al., 2001)

The TMU comprises the crystalline basement of south Hungary, east Croatia, north Serbia, and west Transylvania (Romania) (Haas, 2001). This basement is covered by thick Miocene–Pliocene sediments. During the Neogene the Pannonian Basin underwent a complex tectonic evolution that modified the original Variscan structures of the area.

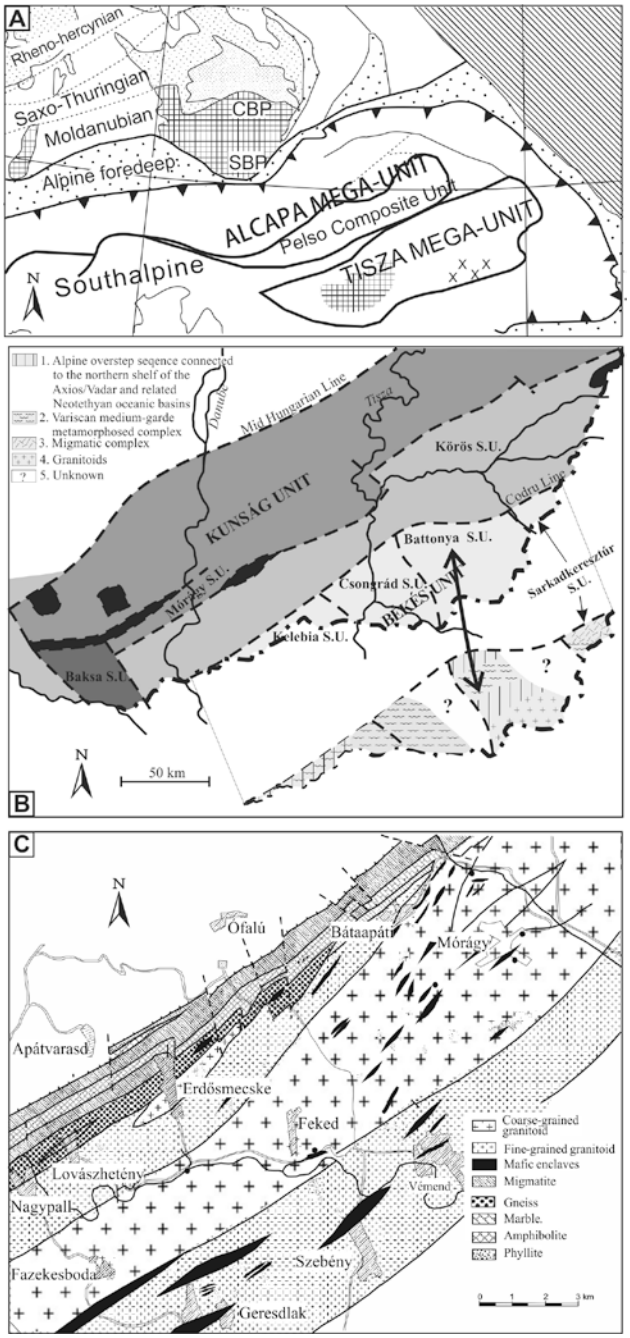

Figure 1. A – Sketch map of the main tectonic units of Central Europe (CBP= Central Bohemian Pluton, SBP=South Bohemian Pluton); B – Pre-Tertiary regional structural map of the Hungarian part of the Tisza-Mega Unit. Inset: simplified geological map of Békés Unit showing the Variscan granitoids of Battonya Subunit after Pál-Molnár et al. (2001); C – Geological sketch map of Variscan granitoids of Mórágy Subunit.

Separation from the Moldanubian Zone of Variscan Europe started in the Late Triassic–Early Cretaceous, as recorded by crystalline rocks and sedimentary sequences (Haas & Péró, 2004; Csontos & Vörös, 2004; Schmid et al., 2008; Buda et al., 2010). As an independent unit the TMU existed from the Late Cretaceous, when its rotation began,

until the Early Miocene (Csontos, 1995; Márton, 2000, 2001).

The Hungarian part of the TMU is divided into the Kunság Unit (KU) and Békés Unit (BU, Haas 2001, Fig. 1/B). The greatest portion of the KU is also covered by sediments, and it outcrops only in the eastern part of Mecsek Mountains in the Mórágy Subunit. The BU can be divided into four subunits: Kelebia, Csongrád, Battonya, and Sarkadkeresztúr. Battonya Subunit is a 15–25 km long, 10–15 km wide body forming a flat anticline covered by 1000–1500 m thick Miocene and Pannonian sediments.

In the Hungarian part of the Variscan TMU, two types of granitoid plutons may be distinguished: an older (340 Ma), deep-seated, metaluminous and slightly peraluminous, K- and Mg-rich, I- and allanite-type granitoid with K-Mg-rich basic durbachitic enclaves occurring in the southwest part of the TMU outcropping in Mórágy Subunit (Mecsek Mts, Fig. 1/C), and a younger (300–330 Ma), mostly strongly peraluminous, S- and monazite-type granitoid in the southeastern part of the TMU located in the Battonya Subunit (Fig. 1/B).

3. SAMPLING AND ANALYTICAL METHODS

The samples from Mórágy Subunit were collected from outcrops, boreholes, and tunnels. A limited number of samples were obtained from the boreholes from Battonya Subunit around Battonya, Mezőhegyes, Pitvaros, and Kunágota settlements. These rocks were acquired from the rock collection of the Department of Mineralogy, Geochemistry, and Petrology of the University of Szeged.

The major element analyses of the rocks were carried out by the inductively coupled plasma atomic emission spectrometry (ICP-AES) method (lower detection limit for major components: 0.01 wt%); FeO content was determined by a titrimetric method and H_2O^- and H_2O^+ by a gravimetric method; inductively coupled plasma mass spctrometry (ICP-MS) was used for trace element analyses (lower detection limits were 0.5 or 0.03 g/t). Analyses were executed by ALS Chemex in Canada (Vancouver).

REE minerals were analysed by the wavelength dispersive spectrometers of an electron microprobe analyser (EMPA, type JXA-733, JEOL). The analytical conditions were an accelerating voltage of 20 kV, a 40–60 nA electron beam current defocused to 3–10 μm, and a counting time of five times of 5 s. For REE analysis the backgrounds were determined by parabolas fitted to peakless ranges of the X-ray spectra; line overlaps were taken into consideration by overlap factors determined during standardization (Nagy, 1993). Y and most REE were measured by their L_α lines; Pr and U by their L_β lines. Glass standards of Drake & Weill (1972) were used for REEs, Y-Al-garnet for Y in xenotime-(Y), oxide for Th, pure metal for U, and mineral standards from Taylor Co. for Si, Ti, Al, Fe, Mn, Mg, Ca, P, and F. The matrix effects were corrected by the classical ZAF method. The detection limits and typical analytical uncertainties are similar to those of Casillas et al., (1995).

4. CHARACTERS OF HOST GRANITOIDS

4.1. Mórágy Subunit

The main granitoid body has magnesio-potassic, met- to peraluminous (ASI≈1.00) character and belongs to the calc-alkaline (A/NK≈1.56), K-rich monzonitic series. It is K, Ca, and Mg enriched whereas Al and Si contents are comparatively low (D≈1.26; Fig. 2).

These rocks are microcline megacryst-bearing amphibole-biotite quartz-monzonite and biotite monzogranite. The maximum microclines occur as megacrysts and as small crystals in the groundmass (medium triclinicity) and have white and pinkish colour. Plagioclase is mostly zoned (An_{35-28}), quartz forms knots with mostly undulatory extinction, and hornblende and actinolite are common in amphibole quartzmonzonite. The hornblende and biotite are rich in Mg [$Fe/(Fe+Mg)_{bi}$ = 0.48, 0.37_{horn}].

The granitoid body contains several highly potassic, metaluminous (ASI≈0.77, A/NK≈1.53, D≈1.92; Fig. 2) mafic enclaves (melamonzonite, melasyenite, locally named durbachite). Amphibole forms “pilites” with tiny chromite grains or occurs as an uralitization product of ferrodiopside. The biotite as well as the amphibole is rich in Mg (0.40_{bi}, 0.29_{horn}) compared with the host granitoid. The plagioclase is andesine (An_{30-40}), sometimes “spike” zonation can be observed (An_{35-45}, spike: An_{60}), and microcline phenocrysts are rare.

A high amount of allanite-(Ce) occurs in addition to apatite, and there is titanite in the enclaves as well as in the enclosing granitoids (Buda et al., 2010) due to the high Ca activity. A high concentration of Ca in melt is known to increase the stability field of allanite-(Ce) **(**Johannes & Holtz 1996).

Allanite-(Ce) is the major REE-rich mineral which controls the condrite normalised REE patterns of the whole-rock (rocks: $\Sigma REE_{encl.}$≈450 g/t, Eu_N/Eu_N^*≈0.60, $\Sigma REE_{gran.}$≈270 g/t, Eu_N/Eu_N^*≈0.75). At the border between granitoid and enclave, hybrid rock (monzonite) occurs with a high content of

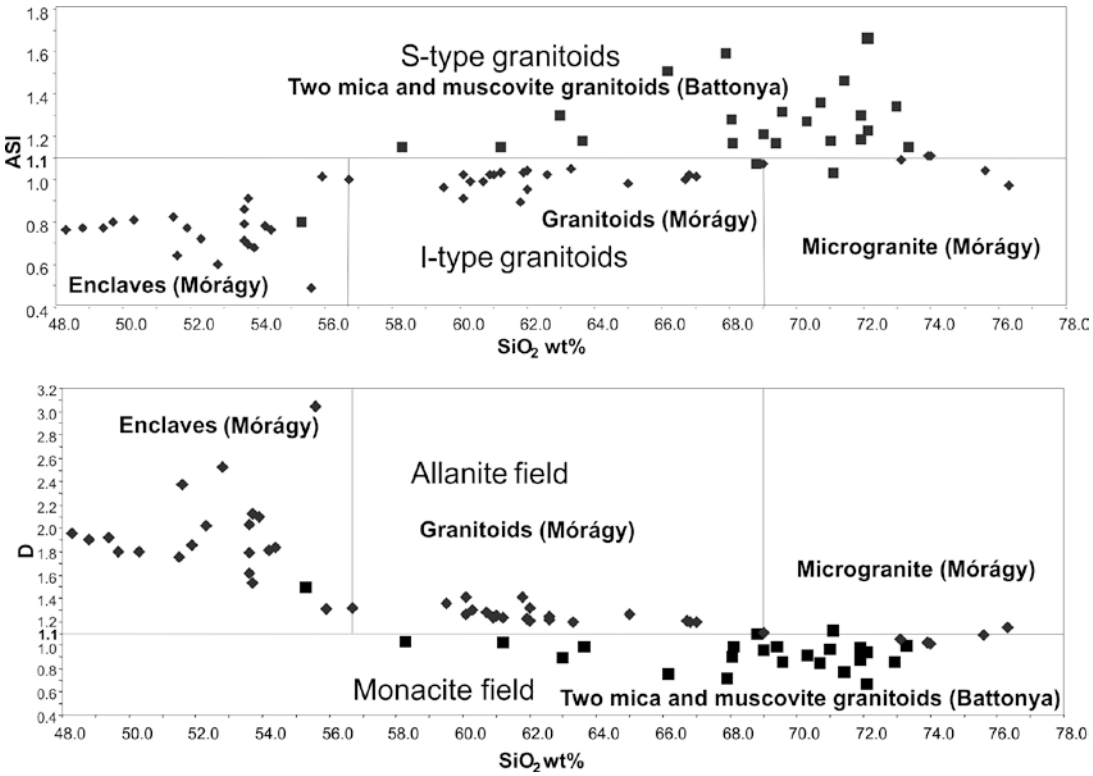

Figure 2. ASI [$Al_20_3/(CaO+Na_20+K_20)$] *v.* SiO_2 and D [(Na+K+Li+2Ca)/Al*1/(Si+Al)], Montel, 1993) *v.* SiO_2 in granitoids of TMU (♦ granitoids of Mórágy Subunit, ■ granitoids of Battony Subunit)

microcline and amphibole (ASI=0.91, A/NK=1.49) and with very high ΣREE content (800 g/t) as a result of abundant allanite-(Ce) with LREE enrichment showing a negative Eu anomaly (Eu_N/Eu_N^*=0.47).

The whole pluton is transected by slightly peraluminous microgranite dikes (ASI≈1.06, A/NK ≈1.26, D≈1.06, Fig. 2). Allanite-(Ce) was not identified in these dikes but monazite-(Ce) occurs. ΣREE content is low (110 g/t), the negative Eu anomaly (Eu_N/Eu_N^*≈0.33) is large, and the ΣLREE/ΣHREE ratio is the lowest among the three rock types (La_N/Yb_N=10; Buda & Pál-Molnár, 2012).

The alteration (microclinization, albitization, chloritization, sericitization, REE fluorcarbonates, and epidote crystallization) and tectonic deformation (schistosity, mylonitization, etc.) are widespread in the igneous body.

The basic (enclaves) and acidic (granitoids) melts probably crystallized at the same time. The basic melt originated from the upper mantle, and the acidic melt formed by partial melting of the continental crust (Buda & Dobosi, 2004).

4.2. Battonya Subunit

These granitoid plutons have a slight thermal contact zone and are surrounded by regional metamorphic rocks and partly covered by Alpine sequences. Generally they are medium-grained equigranular, sometimes with pinkish microcline megacrysts. The majority contain biotite and/or muscovite. The following rock types have been distinguished:

I. Amphibole quartzmonzodiorite is greenish grey, metaluminous (ASI≈0.98, D≈1.49; Fig. 2). Amphiboles form large euhedral to subhedral crystals and also occur as aggregates. The large amphiboles are zoned; the core is Mg-hornblende and the rim is actinolite. Biotite is subhedral and Mg-rich [Fe/(Fe+Mg)=0.31], having a calc-alkaline (Abdel-Rahman 1994) chemical character, and sometimes anhedral in amphibole showing replacement texture. Alteration of biotite to chlorite is common. Primary muscovite is absent and secondary white mica (sericite) is common in plagioclase. The plagioclase has oscillatory zoning varying between oligoclase (An_{17-13}) and andesine (An_{43-40}) with secondary albitization and sericitization. Sometimes they are unzoned oligoclase (An_{17-10}). Cross-hatched microcline shows replacement texture without perthitic exsolution. Quartz is rare and deformed with wavy extinction. Secondary calcite is also present. Accessory minerals are acicular apatite, zircon, and very rare monazite-(Ce). This rock has high ΣREE (≈250 g/t, La_N/Yb_N=19) and a rather low negative Eu-anomaly (Eu/Eu*=0.91). It probably occurs as enclaves in the main peraluminous granitoid pluton.

II and III. Granodiorite and granite are grey with biotite and muscovite or only with muscovite, and sometimes they contain microcline megacrysts. They are strongly peraluminous (ASI≈1.3, corundum $_{CIPW}$=4, D≈0.9; Fig. 2). Biotite is Fe-rich [Fe/(Fe+Mg)=0.58] and strongly pleochroic, with peraluminous (Pál-Molnár et al., 2001) chemical character, sometimes entirely altered to chlorite. Euhedral or subhedral large primary muscovite is common. In some areas it has grown across the biotite, suggesting later crystallization from Al-rich water-saturated melt. The plagioclase sometimes has oscillatory zoning. The cores are mostly oligoclase (An_{25-10}) and the rims are albite (An_{10-0}). The cores are strongly sericitized, altered to clay minerals, or partly replaced by crossed-hatched microcline and albite. Albite and microcline (Or_{97}) are widespread, occurring in replacement textures. Maximum microcline occurs as megacrysts without perthitic exsolution. Quartz is ubiquitous with wavy extinction. Stubby apatite, zircon, and monazite-(Ce) are common accessory minerals. The REE-rich minerals are monazite-(Ce) and a few grains of xenotime-(Y). Muscovite granite has low ΣREE content (90 g/t) with a negative Eu anomaly (Eu/Eu*=0.62–0.93, La_N/Yb_N=13). The REE patterns are controlled by zoned monazite-(Ce).

The majority of the Battonya granitoids are peraluminous (ASI>1) two-mica granodiorite and granite. They are S-type and belong to the calc-alkaline granodioritic series. The amphibole quartzmonzodiorite enclaves are metaluminous. Granitoids formed from the melting of "wet" crustal rocks where two continental lithospheres underplated after the collision.

5. ALLANITE-(Ce) IN GRANITOIDS OF MÓRÁGY SUBUNIT

The amphibole-bearing enclave, the hybrid rock, and the granitoid are very rich in titanite, allanite-(Ce), apatite, and zircon. The granitoids without amphibole do not contain titanite. The microgranite dikes contain garnet, apatite, zircon, and some monazite-(Ce).

Allanite-(Ce) is the most important REE-bearing mineral in the intrusion and controls the REE distribution of the host rock (Buda & Nagy, 1995). It is usually euhedral and zoned, sometimes twinned, and mostly metamict. The grain size is between 2 and 0.5 mm. Inclusions of apatite, amphibole, biotite, feldspars, and quartz are common, indicating that they grew during the entire magmatic crystallization. Allanite-(Ce) in ca 95 wt% is considered to be unaltered (fresh), and that with a lower total is regarded as altered.

The unaltered allanite-(Ce) is rich in REE (ΣREE_2O_3~20–30 wt%, ΣREE: $average_{n68}$: 0.761 pfu: $enclaves_{n15}$=0.752, $hybrid_{n11}$: 0.809, $granitoids_{n42}$: 0.751; see some representative analyses in Table 1) and and low in Al content (average=ΓAl_{n68}: 1.693 pfu, $enclaves_{n15}$: 1.624, $hybrid_{n11}$: 1.687, $granitoids_{n42}$: 1.719) corresponding with allanite-(Ce) occurring in metaluminous granitoids (Petrik et al., 1995). According to Exley (1980), the ΣREE and Al content of allanite-(Ce) has a rather wide range from REE-bearing epidote (clinozoisite) to REE-rich allanite-(Ce) with ΣREE between 0.019 and 0.967 pfu and Al between 1.14 and 2.28 pfu. The oxidation rate of unaltered allanite-(Ce) [$f=Fe^{3+}/(Fe^{2+}+Fe^{3+})$] is between 0.48 and 0.28 (Fig. 3), or, according to Poitrasson's (2002) equation [$f=(\Sigma REE+Th^{4+}/Al^{3+})+1$] are 0.38 (enclaves=0.43, hybrid=0.36, granitoid=0.37), which corresponds with the oxidation rate of I-type magmatic allanites (Fe^{3+}/Fe^{tot}≈0.4; Broska et al., 2000).

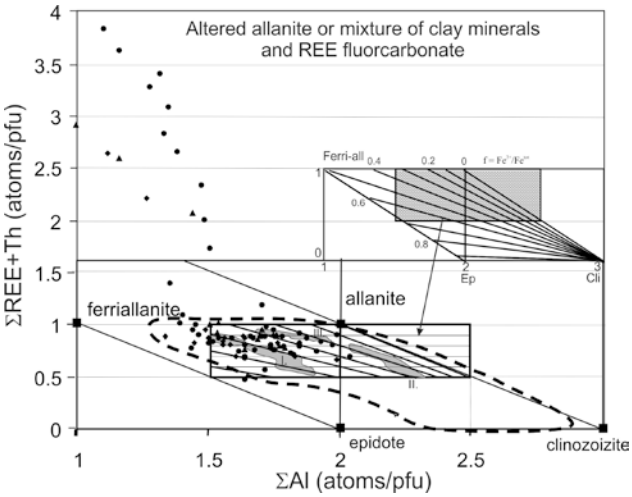

Figure 3. ΣREE/pfu+Th/pfu – ΣAl/pfu in allanite-(Ce) all types of Mecsek granitoids (I. I-type, II. S-type, III. A-type granitoids after Petrik et al.,1995)
● enclaves, ▲ hybrid, ■ granitoid

Altered allanite-(Ce) is enriched in REE (ΣREE_2O_3~40–60 wt%, ΣREE between 1.7 and 3.9/pfu) and depleted in Al, Si, and Ca (Table 2). Metamict grains are common and are surrounded by radial cracks due to volumetric expansion. The crystals are sometimes overgrown by epidote. Usually they are altered, showing dark red colour, sometimes with second-order greenish blue interference colour. Alteration products are REE fluorcarbonates [bastnäsite-(Ce), parisite-(Ce)], thorite, and clay minerals. The low totals (<95 wt %) indicate the incorporation of water, besides carbonate.

Three types of alterations may be distinguished:

1. Complex metamict euhedral grain with a

Table 1. Representative microprobe analyses of allanites from Mórágy Subunit

	Enclaves		Hybride	Granitoid			
	1	2	3	4	5	6	7
SiO_2	34.30	32.75	33.03	32.95	33.98	32.12	32.14
TiO_2	1.38	1.47	1.15	1.26	1.27	1.27	1.10
ThO_2	1.73	1.30	2.10	1.23	1.74	1.18	1.18
UO_2	0.09	0.06	0.06	0.07	0.08	0.09	0.10
Al_2O_3	14.29	15.15	14.80	15.40	14.91	15.30	15.05
Y_2O_3	0.00	0.12	0.04	0.15	0.08	0.17	0.51
Ce_2O_3	10.54	11.92	10.67	13.52	11.58	12.08	11.70
La_2O_3	6.08	5.75	5.59	7.41	6.12	6.11	5.21
Pr_2O_3	0.96	1.11	0.96	1.20	1.01	1.04	1.14
Nd_2O_3	2.83	3.83	2.68	3.74	3.28	3.37	3.96
Sm_2O_3	0.28	0.39	0.30	0.42	0.74	0.47	0.63
Gd_2O_3	0.59	0.35	0.41	0.45	0.42	0.30	0.45
Dy_2O_3	0.01	0.20	0.17	0.01	0.01	0.10	0.22
Eu_2O_3	0.05	0.05	0.02	0.00	0.02	0.01	0.01
Er_2O_3	0.05	0.00	0.12	0.00	0.00	0.00	0.04
FeO	10.31	9.77	10.37	9.75	8.74	12.51	12.62
MnO	0.53	0.40	0.52	0.31	0.42	0.16	0.13
MgO	1.20	1.30	0.67	1.71	1.04	1.39	1.28
CaO	11.56	9.93	10.57	9.16	11.40	10.19	10.21
SrO	0.30	0.00	0.73	0.00	0.25	0.00	0.00
Total	97.08	95.85	94.96	98.74	97.09	97.86	97.68
F	0.35	n.d.	n.d	0.11	0.33	n.d.	n.d.
-O=F2	-0.14	0.00	0.00	-0.05	-0.14	0.00	0.00
CTotal	97.29	95.85	94.96	98.80	97.28	97.86	97.68
	12.5 (O)						
	T						
Si	3.220	3.146	3.189	3.124	3.210	3.052	3.065
	M2						
Al	1.000	1.000	1.000	1.000	1.000	1.000	1.000
	M1+M3						
Ti	0.097	0.106	0.084	0.090	0.090	0.091	0.079
Al	0.580	0.714	0.683	0.719	0.659	0.712	0.690
Fe^3	0.328	0.231	0.300	0.172	0.229	0.299	0.316
Fe^2	0.437	0.528	0.504	0.581	0.436	0.661	0.655
Mg	0.168	0.186	0.096	0.242	0.146	0.197	0.182
Sum	1.610	1.765	1.667	1.804	1.560	1.960	1.922
	A1						
Ca	1.000	1.000	1.000	0.930	1.000	1.000	1.000
	A2						
Ca	0.163	0.022	0.093	0.000	0.154	0.037	0.043
Mn	0.042	0.033	0.043	0.025	0.034	0.013	0.011
Y	0.000	0.006	0.002	0.008	0.004	0.009	0.026
Sr	0.016	0.000	0.041	0.000	0.014	0.000	0.000
U	0.002	0.001	0.001	0.001	0.002	0.002	0.002
Th	0.037	0.028	0.046	0.027	0.037	0.026	0.026
Ce	0.362	0.419	0.377	0.469	0.400	0.420	0.408
La	0.210	0.204	0.199	0.259	0.213	0.214	0.183
Pr	0.033	0.039	0.034	0.041	0.035	0.036	0.040

Table 1. (continued)

	Enclaves		Hyb.	Granitoid			
	1	2	3	4	5	6	7
Nd	0.095	0.131	0.092	0.127	0.111	0.114	0.135
Sm	0.009	0.013	0.010	0.014	0.024	0.015	0.021
Gd	0.018	0.011	0.013	0.014	0.013	0.009	0.014
Dy	0.000	0.006	0.005	0.000	0.000	0.003	0.007
SumA2	1.592	1.575	1.566	1.754	1.689	1.568	1.547
SREE (oxid)	21.390	23.600	20.920	26.750	23.180	23.480	23.360

1 – 4.28/14; 2 – 17. Üh-1, 104m/3; 3 – 12a3/4; 4 – 9/1; 5 – 9/1/4; 6 – Erdősm. D-7/1; 7 – Erdősm. D-7/5. Remarks: first part = sample locality, second part = analysed point

Table 2. Representative microprobe analyses of altered allanites from Mórágy Subunit

	Enclaves		Hybride		Granitoids		
	1	2	3	4	5	6	7
SiO_2	14.41	18.29	12.89	18.99	10.54	11.31	12.14
TiO_2	0.80	0.67	0.32	1.67	1.47	0.96	0.07
ThO_2	2.41	4.59	3.30	2.30	2.87	1.85	0.17
UO_2	0.11	0.01	0.22	0.01	0.29	0.34	0.29
Al_2O_3	4.54	7.60	5.21	9.33	5.63	6.50	2.35
Y_2O_3	0.00	0.21	0.00	0.00	0.15	0.22	0.08
Ce_2O_3	28.55	18.87	20.86	19.70	27.04	25.86	30.95
La_2O_3	15.85	9.86	18.02	12.47	14.16	13.50	16.84
Pr_2O_3	2.35	1.76	1.98	1.62	2.63	2.60	2.90
Nd_2O_3	7.43	7.08	4.53	5.28	8.54	8.49	10.60
Sm_2O_3	0.73	0.70	0.28	0.54	1.08	1.06	1.00
Gd_2O_3	1.34	0.76	0.44	0.63	0.57	0.59	0.55
Dy_2O_3	0.00	0.06	0.00	0.00	0.04	0.06	0.01
Eu_2O_3	0.01	0.02	0.00	0.00	0.01	0.04	0.60
Er_2O_3	0.00	0.00	0.00	0.00	0.00	0.00	0.00
FeO	3.38	4.78	5.13	6.77	1.06	1.35	0.39
MnO	0.08	0.20	0.17	0.28	0.02	0.06	0.01
MgO	0.28	0.67	3.22	0.39	0.05	0.31	1.22
CaO	6.44	7.30	4.35	7.51	4.96	4.92	3.98
SrO	0.37	0.00	0.15	0.47	0.00	0.00	0.00
Total	89.08	83.43	81.07	87.96	81.11	80.02	84.15
F	5.26	n.d.	n.d.	n.d.	5.20	5.24	6.05
-O=F2	-2.21	0.00	0.00	0.00	-2.19	-2.21	-2.55
CTotal	92.13	83.43	81.07	87.96	84.12	83.05	87.65
SREE(oxid)	56.26	39.11	46.11	40.24	54.07	52.20	63.45

1 – 28/15; 2 – Üh-1, 104m/1; 3 – 12a2/4; 4 –12a3/4; 5 – Erdősmecske/10; 6 – Same/4; 7 – Same/15. Remarks: first part= sample locality, second part= analysed point

zoned metamict core overgrown with unzoned metamict allanite-(Ce) and surrounded by a thin ΣREE-rich rim (REE fluorcarbonate); see figure 4. In the crystal core, from core to rim of the core crystal the ΣREE shows positive correlations with U (r=0.8), Th (r=0.6), and F (r=0.9) and negative correlations with Si (r = –0.9), Al (r = –0.9), and Fe (r = –0.6) (Fig. 4).

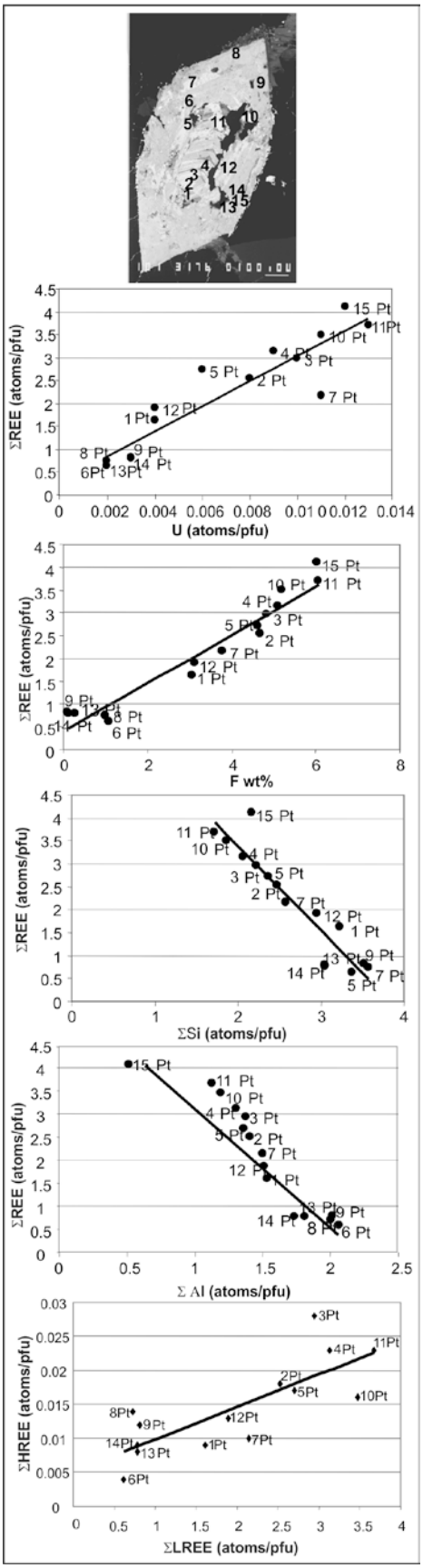

Figure 4. Backscattered electron (BSE) image and compositional diagrams of complex euhedral allanite-(Ce), with altered REE-rich zoned core and unaltered zone with thin REE-rich rim (hardly seen in the image) from granitoid (numbers are the analyzed points)

Ca has no direct correlation with ΣREE but generally it also decreases with increasing ΓREE content. ΣHREE as well as ΣLREE are enriched (LREE and HREE, r=0.8) toward the edge of the core crystal. Lower totals are probably due to OH^- and CO_3^{-2}. In the crystal cores, Si, Al, and (Fe) were leached by solution with higher pH, and REE, Th, and U distributions probably reveal the original in situ "magmatic" zonation. The cores were later overgrown by second generation of allanite (Fig. 4.), and finally some REE-rich mineral precipitated at the very edge as REE fluorcarbonate.

2. Inside the crystals irregular REE-rich or -poor patches or zones are common (Plate 1, a, b, c).

3. The rim is depleted irregularly in ΣREE, Fe, Mn, and Mg, sometimes with occurrence of secondary thorite (Plate 1, d, e, f).

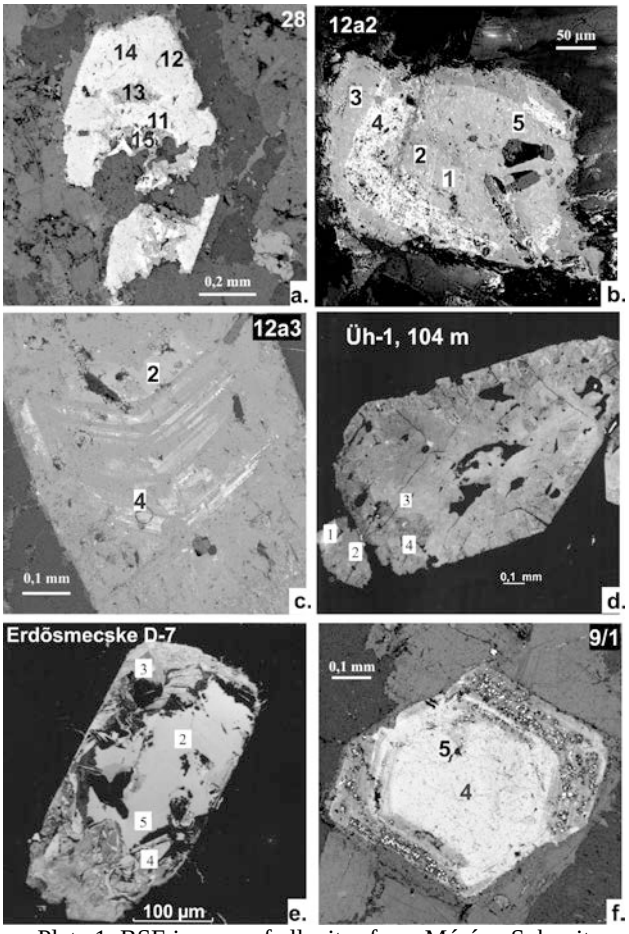

Plate 1. BSE images of allanites from Mórágy Subunit a. Euhedral partly altered crystal in enclave (unaltered (11, 12, 14) and altered (15) crystals; b. Altered zone (4) within unaltered allanite (1,2,3,5) in hybrid rock; c. Altered zones (4) in the middle of the unaltered crystal in hybrid rock; d. Large euhedral unaltered (3) and altered fragment (1) of allanite in enclave; e. Unaltered euhedral crystals (5) with irregularly altered rim in granitoids; f. thorite inclusions (small white grains) in the altered rim of the crystal in granitoids (numbers in brackets are microprobe analyses in the Table 1, Table 2 or in the data base).

Leaching of different components of allanite-(Ce) can be explained by changes in the pH of the solutions. Basic (peralkaline) solutions (originated from K-metasomatism or alteration of Na-rich feldspar) leached Si and Al, while acidic fluids (e.g. aggressive carbonic and hydrofluoric acids with pH=4–5) mobilized the REE and Th as carbonate (CO_3^{-2}) or hydroxide (OH^-) complexes or free ions, which were precipitated as REE (fluor) carbonate [bastnäsite-(Ce), parisite-(Ce)] and thorite, according to Nesbitt (1979). REE-rich zones occurring within allanite-(Ce) crystals are presumably sub-micron intergrowths of allanite-(Ce) with bastnäsite-type mineral phases (Zakrzewski et al., 1992) or REE fluorcarbonate and clay minerals.

6. MONAZITE-(Ce) IN GRANITOIDS OF BATTONYA SUBUNIT

The main granitoids are Al-rich two-mica and muscovite granodiorite-granite where ASI is >1.1 and D<1. Only monazite-(Ce) occurs as a REE-rich mineral in these rocks. Due to the high Al and low Ca, only monazite-(Ce) can occur (Montel, 1993). In amphibole quartzmonzodiorite enclaves, ASI<1 and D~1.5, contain low amount of monazite-(Ce).

Monazite-(Ce) sizes vary from a few micrometres to ~ 300 μm. They are generally euhedral or subhedral but rounded grains are also common. The following textural types were distinguished: 1. monazite-(Ce) inclusions in zircon (Plate 2, a). 2. zircon inclusions in monazite-(Ce) and intergrown with zircon (Plate 2, b, c). 3. monazite and/or zircon inclusions in apatite and intergrowth (Plate 2, d, e, f, Plate 3, a, b). 4. apatite and biotite inclusion in monazite-(Ce) (Plate 3, c, d). These textural relations indicate that monazite-(Ce) crystallization was continuous during the solidification of the granitoid melt. Zoned monazite-(Ce) crystals are common, with normal (increasing HREE towards the rim) as well as oscillatory zonation (Plate 2, e, Plate 3, e, f).

Xenotime-(Y) is rather rare and is sometimes intergrown with monazite-(Ce) and sometimes euhedral (Plate 3, g). It occurs in two-mica granitoids.

Chemistry of monazite-(Ce): Monazite-(Ce) in quartzmonzodiorite is rich in Ca, which corresponds with higher Ca content of the host rock (Table 3). A slight enrichment of HREEs (0.10 pfu) can be detected in monazite-(Ce) from granitoids compared with q-monzodiorite (0.089 pfu). The negative correlation of LREEs versus HREEs is good ($-0.74_{n=25}$). Compositions are approximately $Mo_{87\text{-}96}Hu_{2\text{-}4}Ch_{4\text{-}12}$ (Ca=0.087–0.049 pfu, Th=0.042–0.038 pfu; Fig. 5).

Chondrite-normalized diagrams show negative Eu anomalies. The high fluctuation and differences in the HREE field are apparently analytical uncertainties (Fig. 6).

7. SUMMARY

Unaltered and altered varieties of allanite-(Ce) are very common in the Variscan granitoids of Mórágy Subunit and govern the host-rock chondrite-normalized REE distributions. High oxidation of the unaltered allanite-(Ce) indicates that it crystallized under high oxygen fugacity from the I-type high temperature granitoid melt. The crystallization was continuous during the solidification of the rock as evidenced by abundant rock-forming mineral inclusions. The presence of allanite-(Ce) is caused by the low Al and high Ca contents of the host melt. The ΣHREE content of allanite-(Ce) is three times higher in the granitoid than in the enclaves.

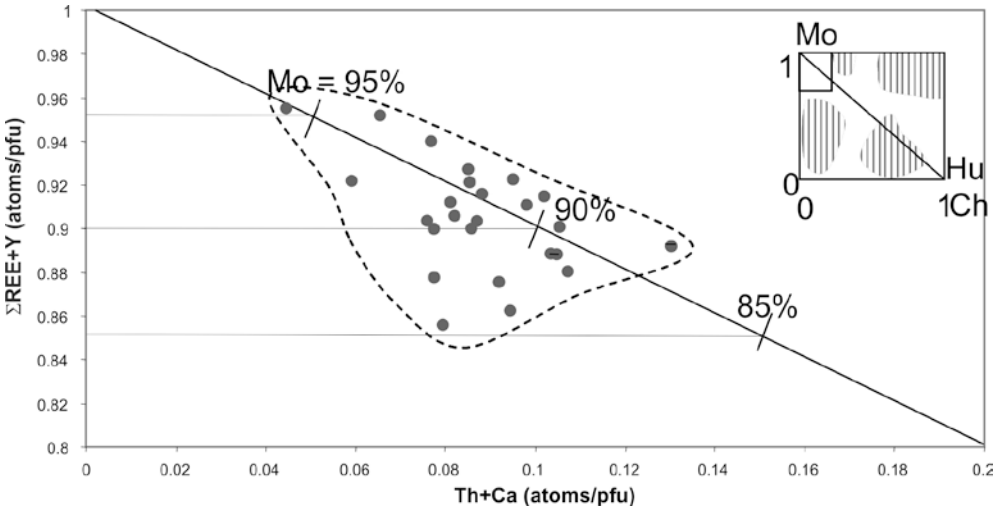

Figure 5. Composition of monazite-(Ce) in ΓREE+Y/pfu – Th+Ca/pfu diagram after Broska et al., 2000

Table 3. Representative microprobe analyses of monazite-(Ce) and xenotime-(Y) from Battonya granitoids

	A	**Two mica granitoid**																**Muscovite granitoid**					**B**
	1.	**2.**			**3.**			**4.**									**5.**				**6.**	**7.**			**8.**	**9.**
ThO_2	4.71	4.86	5.01	6.19	3.39	2.06	4.36	4.66	4.26	4.51	2.79	4.19	3.77	5.34	3.78	2.70	5.29	4.20	4.25	4.42	4.34	4.89	4.63	5.10	4.39	0.11
P_2O_5	29.52	30.94	29.00	28.21	30.91	29.83	29.94	30.63	29.86	29.53	29.32	29.25	29.30	29.16	29.06	27.78	29.59	30.14	29.82	29.49	30.21	30.36	29.70	30.42	29.95	33.88
Y_2O_3	0.83	2.92	0.31	0.56	1.71	2.27	2.17	0.54	0.51	0.82	0.67	0.68	0.48	0.80	0.37	1.06	1.30	0.22	0.63	0.52	0.69	0.30	0.71	0.85	0.38	42.43
CaO	2.07	1.26	0.93	1.05	1.20	0.96	1.13	1.26	1.17	1.37	0.99	1.34	1.30	1.36	1.01	0.47	1.31	0.91	0.98	1.08	1.05	1.49	0.84	1.52	0.99	0.24
UO_2	0.11	1.70	0.10	0.06	2.62	1.43	1.09	0.10	0.10	0.40	0.37	0.24	0.33	0.58	0.27	0.41	0.57	0.11	0.17	0.02	0.16	0.04	0.00	0.16	0.04	1.09
Gd_2O_3	1.02	1.88	0.87	1.12	1.48	1.79	1.62	0.86	0.95	1.26	0.91	0.89	0.92	1.34	0.76	1.35	1.78	0.85	1.00	0.55	0.93	0.63	0.74	1.10	1.18	2.23
Sm_2O_3	1.88	2.19	1.53	1.99	2.07	2.53	2.37	1.77	1.72	2.33	1.86	2.01	1.85	2.40	1.77	2.36	2.73	1.79	1.89	1.73	1.86	1.63	1.90	2.03	2.03	0.70
Nd_2O_3	12.41	10.67	11.22	12.34	11.15	11.31	11.74	12.44	12.66	12.68	12.27	12.24	11.93	12.89	12.68	12.36	12.74	13.16	11.86	12.67	11.93	11.73	12.99	12.76	12.59	0.49
Pr_2O_3	3.24	3.07	3.23	3.28	2.98	3.34	3.18	3.07	3.14	3.31	3.16	3.19	3.13	3.37	3.22	3.18	3.24	3.43	3.27	3.38	3.32	2.94	3.27	3.19	3.44	0.10
Ce_2O_3	30.25	28.15	32.72	30.70	28.48	28.90	28.60	31.17	31.11	29.73	31.26	30.44	30.57	29.20	31.40	30.99	28.64	30.84	30.64	32.06	32.08	31.44	30.65	30.35	31.45	0.20
La_2O_3	12.56	11.80	13.96	12.40	12.07	13.47	12.96	12.90	13.45	13.29	15.75	14.10	15.34	12.87	15.23	14.37	11.12	12.89	13.42	13.27	13.09	14.35	12.37	12.36	12.66	0.00
Tb_2O_3	0.01	0.12	0.00	0.01	0.04	0.10	0.08	0.00	0.00	0.00	0.01	0.02	0.01	0.04	0.00	0.06	0.11	0.00	0.06	0.00	0.00	0.00	0.02	0.03	0.00	0.54
Ho_2O_3	0.00	0.00	0.00	0.00	0.00	0.06	0.00	0.00	0.00	0.12	0.06	0.01	0.01	0.02	0.01	0.00	0.00	0.00	0.00	0.00	0.00	0.00	0.00	0.00	0.00	1.29
Dy_2O_3	0.19	0.81	0.05	0.17	0.56	0.77	0.66	0.13	0.04	0.26	0.27	0.22	0.27	0.29	0.10	0.46	0.44	0.00	0.27	0.08	0.14	0.04	0.17	0.24	0.17	5.65
Er_2O_3	0.00	0.13	0.00	0.02	0.14	0.10	0.09	0.00	0.00	0.01	0.00	0.00	0.05	0.01	0.01	0.03	0.03	0.00	0.00	0.00	0.00	0.00	0.00	0.01	0.00	3.90
Tm_2O_3	0.00	0.00	0.00	0.00	0.00	0.15	0.07	0.00	0.00	0.21	0.09	0.06	0.00	0.15	0.05	0.07	0.00	0.00	0.00	0.00	0.00	0.00	0.00	0.00	0.00	0.73
Eu_2O_3	0.16	0.38	0.15	0.19	0.15	0.10	0.17	0.14	0.19	0.20	0.23	0.21	0.17	0.27	0.18	0.30	0.21	0.12	0.16	0.27	0.22	0.16	0.18	0.20	0.09	0.06
Yb_2O_3	0.00	0.00	0.00	0.00	0.00	0.05	0.00	0.00	0.00	0.05	0.00	0.00	0.00	0.00	0.01	0.01	0.00	0.00	0.00	0.00	0.00	0.00	0.00	0.00	0.00	3.45
Lu_2O_3	0.00	0.00	0.00	0.00	0.00	0.00	0.00	0.00	0.00	0.00	0.00	0.00	0.00	0.00	0.00	0.00	0.00	0.00	0.00	0.00	0.00	0.00	0.00	0.00	0.00	1.11
SiO_2	0.31	0.00	0.31	0.75	0.00	0.09	0.16	0.85	0.59	0.15	0.21	0.07	0.81	0.61	0.56	1.68	0.21	0.22	1.70	0.41	0.37	0.29	0.49	0.40	0.22	0.37
Total	99.27	100.88	99.39	99.04	98.95	99.31	100.39	100.52	99.75	100.23	100.22	99.16	100.24	100.70	100.47	99.64	99.31	98.88	100.12	99.95	100.39	100.29	98.66	100.72	99.58	98.57
	Numbers of ion on the basis of 16 (O)																									
Si	0.049	0.000	0.049	0.121	0.000	0.014	0.025	0.130	0.092	0.024	0.033	0.011	0.127	0.096	0.088	0.267	0.033	0.035	0.261	0.064	0.057	0.045	0.077	0.062	0.035	0.051
P	3.928	4.019	3.914	3.839	4.067	3.970	3.955	3.969	3.945	3.934	3.916	3.939	3.879	3.876	3.877	3.741	3.956	4.013	3.877	3.926	3.970	3.982	3.969	3.970	3.982	3.926
La	0.727	0.667	0.820	0.735	0.691	0.780	0.745	0.727	0.773	0.771	0.916	0.826	0.884	0.745	0.884	0.842	0.647	0.747	0.759	0.769	0.749	0.819	0.719	0.702	0.733	0.000
Ce	1.739	1.579	1.908	1.805	1.619	1.662	1.632	1.745	1.776	1.711	1.803	1.771	1.748	1.676	1.810	1.803	1.654	1.774	1.721	1.844	1.821	1.781	1.769	1.711	1.806	0.010
Pr	0.185	0.171	0.187	0.192	0.169	0.191	0.181	0.171	0.178	0.190	0.181	0.185	0.178	0.193	0.185	0.184	0.186	0.196	0.183	0.193	0.188	0.166	0.188	0.179	0.197	0.005
Nd	0.696	0.584	0.638	0.708	0.618	0.635	0.654	0.679	0.705	0.712	0.691	0.695	0.666	0.722	0.713	0.702	0.718	0.739	0.650	0.711	0.661	0.649	0.732	0.702	0.706	0.024
Sm	0.102	0.116	0.084	0.110	0.111	0.137	0.127	0.093	0.092	0.126	0.101	0.110	0.100	0.130	0.096	0.129	0.148	0.097	0.100	0.094	0.099	0.087	0.103	0.108	0.110	0.033
Gd	0.053	0.095	0.046	0.060	0.076	0.093	0.084	0.044	0.049	0.066	0.048	0.047	0.048	0.070	0.040	0.071	0.093	0.044	0.051	0.029	0.048	0.032	0.039	0.056	0.061	0.101
Y	0.069	0.238	0.026	0.048	0.141	0.190	0.180	0.044	0.042	0.069	0.056	0.057	0.040	0.067	0.031	0.090	0.109	0.018	0.051	0.043	0.057	0.025	0.060	0.070	0.032	3.087
U	0.004	0.058	0.004	0.002	0.091	0.050	0.038	0.003	0.003	0.014	0.013	0.008	0.011	0.020	0.009	0.015	0.020	0.004	0.006	0.001	0.006	0.001	0.000	0.005	0.001	0.033
Th	0.168	0.170	0.182	0.226	0.120	0.074	0.155	0.162	0.151	0.162	0.100	0.152	0.134	0.191	0.136	0.098	0.190	0.150	0.149	0.158	0.153	0.172	0.166	0.179	0.157	0.003
Eu	0.010	0.020	0.010	0.010	0.010	0.010	0.010	0.010	0.010	0.010	0.010	0.010	0.010	0.010	0.010	0.020	0.010	0.010	0.010	0.010	0.010	0.010	0.010	0.010	0.000	0.000
Tb	0.000	0.010	0.000	0.000	0.000	0.010	0.000	0.000	0.000	0.000	0.000	0.000	0.000	0.000	0.000	0.000	0.010	0.000	0.000	0.000	0.000	0.000	0.000	0.000	0.000	0.020
Dy	0.010	0.040	0.000	0.010	0.030	0.040	0.030	0.010	0.000	0.010	0.010	0.010	0.010	0.010	0.010	0.020	0.020	0.000	0.010	0.000	0.010	0.000	0.010	0.010	0.010	0.250
Ho	0.000	0.000	0.000	0.000	0.000	0.000	0.000	0.000	0.000	0.010	0.000	0.000	0.000	0.000	0.000	0.000	0.000	0.000	0.000	0.000	0.000	0.000	0.000	0.000	0.000	0.060
Er	0.000	0.010	0.000	0.000	0.010	0.000	0.000	0.000	0.000	0.000	0.000	0.000	0.000	0.000	0.000	0.000	0.000	0.000	0.000	0.000	0.000	0.000	0.000	0.000	0.000	0.170
Tm	0.000	0.000	0.000	0.000	0.000	0.010	0.000	0.000	0.000	0.010	0.000	0.000	0.000	0.010	0.000	0.000	0.000	0.000	0.000	0.000	0.000	0.000	0.000	0.000	0.000	0.030
Yb	0.000	0.000	0.000	0.000	0.000	0.000	0.000	0.000	0.000	0.000	0.000	0.000	0.000	0.000	0.000	0.000	0.000	0.000	0.000	0.000	0.000	0.000	0.000	0.000	0.000	0.140
Lu	0.000	0.000	0.000	0.000	0.000	0.000	0.000	0.000	0.000	0.000	0.000	0.000	0.000	0.000	0.000	0.000	0.000	0.000	0.000	0.000	0.000	0.000	0.000	0.000	0.000	0.050
Ca	0.349	0.207	0.159	0.181	0.200	0.162	0.189	0.207	0.196	0.231	0.167	0.228	0.218	0.229	0.171	0.080	0.222	0.153	0.161	0.182	0.175	0.247	0.142	0.251	0.167	0.035
Cations	8.069	7.904	8.017	8.027	7.903	7.958	7.965	7.974	8.002	8.010	8.025	8.029	8.033	8.015	8.040	8.022	7.976	7.970	7.969	8.014	7.984	8.006	7.964	7.995	7.987	7.308

A – quartzmonzodiorite; B – xenotime-(Y) two mica granitoid. 1. Battonya-É; 2. Battonya-10; 3. Battonya-37; 4. Battonya-41; 5. Battonya-64; 6. Battonya-12; 7. Battonya-17; 8. Battonya-63; 9. Battonya-37

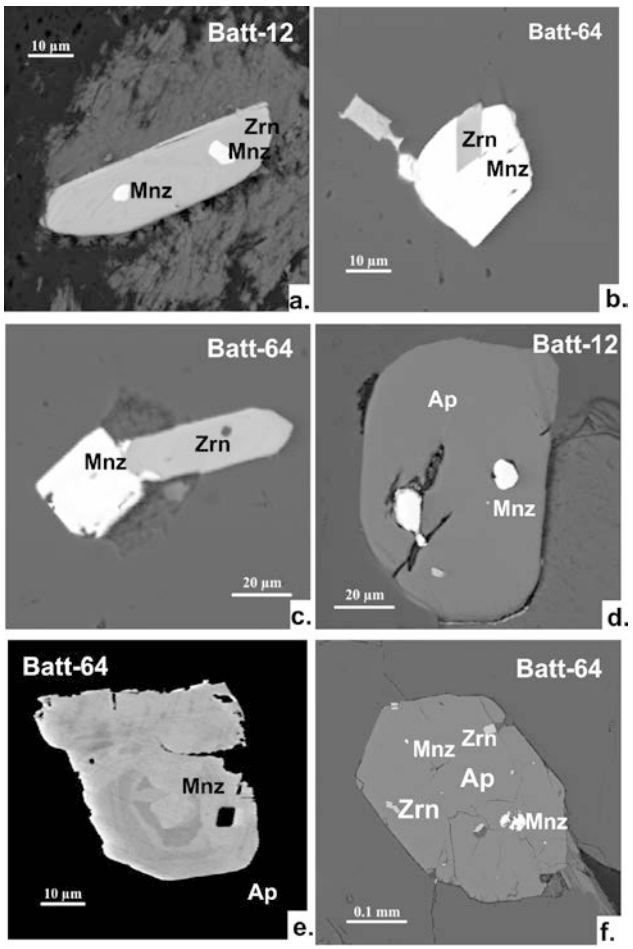

Plate 2. BSE images of accessories of muscovite granitoid from Battonya Subunit
a. Monazite-(Ce) inclusion of zircon; b. Zircon inclusion in monazite-(Ce); c. Monazite-zircon intergrowth; d. Monazite inclusions in apatite; e. Zoned monazite inclusion in apatite; 6. Monazite and zircon inclusions in apatite. Legend: Mnz = monazite; Zrn = zircon; Ap = apatite; Bt = biotite

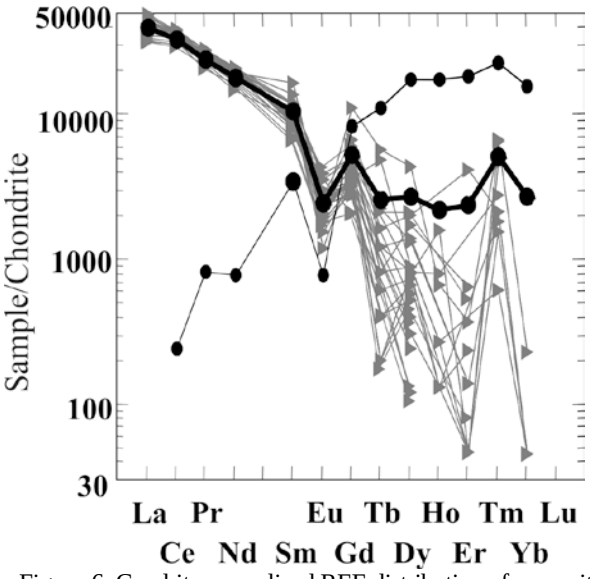

Figure 6. Condrite normalized REE distribution of monazites (▶; average of monazite: dots and thick line) and xenotime-(Y) (●)

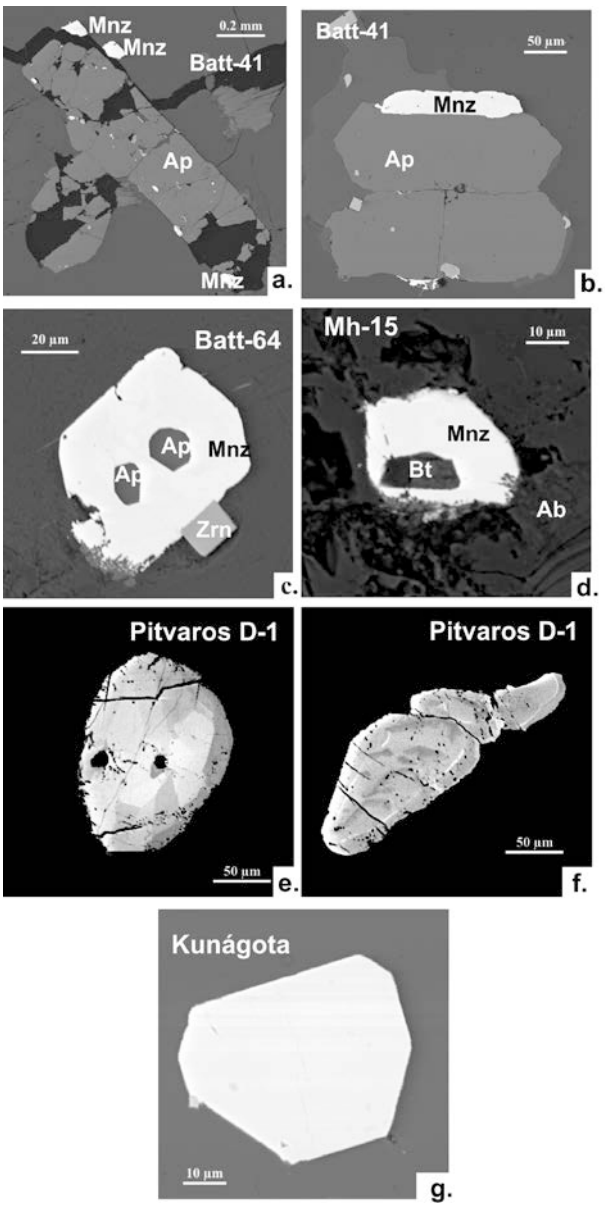

Plate 3. BSE images of accessories of muscovite granitoid from Battonya Subunit
a. Monazite-(Ce) in and at the rim of apatite; b. Monazite and apatite intergrowth; c. Apatite inclusions in monazite; d. Biotite inclusion in monazite; e–f. Zoned monazites; g. Euhedral xenotime-(Y). Legend: Mnz = monazite; Zrn=zircon; Ap = apatite; Bt = biotite

Post-magmatic processes such as hydrothermal solutions altered the allanite-(Ce) in different ways depending on the pH of solutions. Higher pH leached the Si and Al, while lower pH resolved the REE, which were transported and precipitated in the rim of crystals or in nearby cracks as REE-rich fluorcarbonates. Some of the zoned crystals preserved their original magmatic REE zonation, showing higher ΣREE content towards the edge even after the leaching of Al and Si. The changing pH caused secondary allanite-(Ce) and epidote crystallization later on.

Monazite-(Ce) rarely xenotime-(Y) occur in Al-rich, Ca-poor granitoids of Battonya Subunit. Similarly with allanite-(Ce), crystallization of monazite-(Ce) was continuous during solidification of rocks.

8. DISCUSSION AND CONCLUSION

The SiO_2 contents of the host rocks of allanite-(Ce) and monazite-(Ce) have a negative correlations with ΣREE (e.g., ΣREE=450 g/t in basic enclaves, 270 g/t in granitoids, and 110 g/t in microgranite in Mecsek or 250 g/t in quartzmonzodiorite and 90 g/t in muscovite granitoid in Battonya). The La_N/Yb_N ratios also decreases with increasing SiO_2 (Mórágy Subunit: La_N/Yb_N=30 at SiO_2=60 wt% and 10 at SiO_2=76 wt%; Battonya Subunit: La_N/Yb_N=20 at SiO_2=55 wt% and 13 at SiO_2=73 wt %). Decreasing temperature promotes polymerization of Al and Si. This environment is not favoured by ΣREE, and consequently high-SiO_2-content granitoids are depleted in REE (Miller & Mittlefehldt, 1982). With increasing volatiles, LREE go into solution, HREE becomes relatively enriched (Rapp & Watson, 1986) in the rock, and xenotime can crystallize.

Large euhedral allanite-(Ce) occurs in Ca-rich metaluminous enclaves and granitoids of Mórágy Subunit (ASI≈0.8–1.0, D≈1.9–1.3, and CaO=5–2 wt %). Unaltered allanite-(Ce) has considerably lower Th (0.032/apfu), U (0.001/apfu), and La+Ce+Pr (0.656/apfu) compared with allanite-(Ce) showing a different rate of alteration (average Th=0.089/apfu, U=0.007/apfu, La+Ce+Pr=2.453/apfu). The U content increases with ΣLREE (r=0.8), as does Th (r=0.6), but Th can crystallize as small thorite grains in the altered rims of allanite-(Ce). Intense alteration of allanite-(Ce) is due to hydrothermal activity. Alkali-rich fluids due to K-metasomatism and alteration of Na-rich plagioclase dissolve the Si and Al contents of allanite-(Ce), and REE become relatively enriched. The decreasing pH of hydrothermal fluids caused secondary allanite-epidote crystallization or even leaching of REE, and REE fluorcarbonates [bastnäsite-(Ce), parisite-(Ce)] and thorite precipitated from saturated solution. K-metasomatism and hydrothermal alteration are widespread in the I-type granitoid intrusion of Mórágy Subunit.

Small, mostly rounded grains of monazite-(Ce) are ubiquitous in S-type peraluminous granitoids of Battonya Subunit (ASI≈1.0–1.3, D≈0.9, CaO=0.5–1.8wt%). The solubility of monazite-(Ce) is therefore low in the peraluminous melt (SiO_2-Al_2O_3-K_2O-Na_2O); therefore, monazite-(Ce) is common in these two-mica granites (Montel, 1986).

Monazite-(Ce) is enriched in LREE (average La+Ce+Pr: 2.697/apfu). The Th content (0.154/apfu) is 10 times more than the U content (0.015/apfu). U has a weak correlation with LREEs (r=0.6). According to mineral inclusions of monazite-(Ce), its crystallization from the magma was continuous, starting with a higher temperature (monazite-(Ce) inclusions in zircon) and finishing with an alkali volatile-rich low-temperature environment (biotite inclusion in monazite-(Ce)). Local decreasing of the alkali content – due to the previous biotite crystallization – decreases the solubility of monazite-(Ce), and consequently, monazite-(Ce) can crystallize after biotite.

ACKNOWLEDGEMENTS

The project was supported by the Hungarian National Research Fund (OTKA) No. K-67787. The authors are grateful to Ron Fodor and David Watkinson for critical review of the manuscript.

REFERENCES

Abdel-Rahman, A.F.M., 1994. *Nature of biotites from alkaline, calc-alkaline and peraluminous magmas.* Journal of Petrology, 35, 525–541.

Broska, I., Petrik, I. & Williams, C.T., 2000. *Coexisting monazite and allanite in peraluminous granitoids of the Tribeč Mountains, Western Carpathians.* American Mineralogist, 85, 22–32.

Buda, Gy. & Nagy, G., 1995. *Some REE-bearing accessory minerals in two types of Variscan granitoids, Hungary.* Geologica Carpathica, 46, 2, 67–78.

Buda, Gy. & Dobosi, G., 2004. *Lamprophyre-derived high-K mafic enclaves in Variscan granitoids from the Mecsek Mts. (South Hungary).* N. Jb. Miner. Abh., 180, 2, 115–147.

Buda, Gy., Koller, F., András, E. & Nagy, G., 2010. *Hungarian Variscan granitoids and their correlation with surrounding granitoids.* Acta Mineralogica Petrographica Abstract Series, 6, 507.

Buda, Gy. & Pál-Molnár, E., 2012. *Apatite as a petrogenetic indicator of Variscan granitoids in Tisza Mega-Unit (South Hungary).* Carpathian Journal of Earth and Environmental Sciences, 7, 4, 47–60.

Casillas, R., Nagy, G., Pantó, Gy., Brandle, J.L. & Fórizs, I., 1995. *Occurrence of Th, U, Y, Zr, and REE-bearing accessory minerals in late-Variscan granitic rocks from the Sierra de Guadarrama and their petrogenetic significance.* Eur. J. Mineral., 7, 989–1006.

Csontos, L., 1995. *Tertiary tectonic evolution of the Intra-Carpathian area: a review.* Acta Vulcanologica, 7, 1–13.

Csontos, L. & Vörös, A., 2004. *Mesozoic plate tectonics reconstruction of the Carpathian region.* Paleogeogr. Paleoeco., 210, 1–56.

Drake, M.I. & Weill, P.P., 1972. *New rare earth element standards for electron microprobe analysis.* Chem. Geol., 10, 179–181.

Exley, R.A., 1980. *Microprobe studies of REE-rich accessory minerals: implications for Skye granite petrogenesis and REE mobility in hydrothermal systems.* Earth Planet Sci. Letters, 48, 97–110.

Haas, J. (ed.), 2001. *Geology of Hungary.* Eötvös University Press, Budapest, 317 p.

Haas, J. & Péró C., 2004. *Mesozoic evolution of the Tisza Mega-unit.* Int. J. Earth. Sci., 93, 297–313.

Johannes, W. & Holtz, F., 1996. *Petrogenesis and Experimental Petrology of Granitic Rocks. Minerals and rocks.* Springer, 335 p.

Lee, D.E. & Bastron, H., 1967. *Fractionation of rare-earth elements in allanite and monazite as related to geology of the Mt. Weeler mine area, Nevada.* Geochim. et Cosmochim. Acta, 31, 339–356.

Márton, E., 2000: *The Tisza Megatectonic Unit in the light of paleomagnetic data.* Acta Geologica Hungarica, 43, 3, 329–343.

Márton, E., 2001. *Tectonic implications of Tertiary paleomagnetic results from the PANCARDI area (Hungarian contribution).* Acta Geologica Hungarica, 44, 135–144.

Miller, F.C. & Mittlefehldt, D.V., 1982. *Depletion of light rere-earth elements in felsic magmas.* Geology, 10, 129–133.

Montel, J.M., 1986. *Experimental determination of the solubility of Ce-monazite in SiO_2-Al_2O_3-K_2O-Na_2O melts at 800℃, 2 kbar under H_2O-saturared conditions.* Geology, 14, 659–662.

Montel, J.M., 1993. A *model for monazite/melt equilibrium and application to the generation of granitic magmas.* Chemical Geology, 110, 127–146.

Nagy, G., 1993. *Quick method for REE mineral analyses by EPMA.* Int. Conf. on RE-minerals, London, Abstracts, 94–96.

Nesbitt, W., 1979. *Mobility and fractionation of rare earth elements during weathering of a granodiorite.* Nature, 272, 206–210.

Pál-Molnár, E., Kovács, G. & Batki, A., 2001. *Petrographical characteristics of Variscan granitoids of Battonya Unit boreholes (SE Hungary).* Acta Mineralogica-Petrographica, 42, 21–31.

Petrik, I., Broska, I., Lipka, J. & Siman, P., 1995. *Granitoid allanite-(Ce): Subtitution relations, redox conditions and REE distributions (on example of I-type granitoid, Western Carpathians, Slovakia).* Geologica Carpatica, 46, 79–94.

Rapp, R.P. & Watson E.B., 1986. *Monazite solubility and dissolution kinetics: implications for the thorium and light rare earth chemistry of felsic magmas.* Contrib. Mineral. Petrol., 94, 304–316.

Poitrasson, F., 2002. *In situ investigations of allanite hydrothermal alteration: examples from calc-alkaline and anorogenic granites of Corsica (southeast France).* Contrib. Mineral. Petrol., 142, 485–500.

Schmid, S.M., Bernoulli, D., Fügenschuh, B., Matenco, L., Schefer, S., Schuster, R., Tischler, M. & Ustaszewski, K., 2008. *The Alpine-Carpathian-Dinaridic orogenic system: correlation and evolution of tectonic units.* Swiss Journal of Geosciences, 101, 1, 139–183.

Spicer, E., Scheepers, R. & Miller, J., 2006. *Apatite, allanite and monazite as petrogenetic indicators in S-, I- and A-type granites of the Cape Granite Suite, Western Cape Province, South Africa.* Geophysical Research Abstract, 8, 06363.

Zakrzewski, M.A., Lustenhouwer, W.J., Nugteren, H.J & Williams, C.T., 1992. *Rare-Earth Minerals Yttrian Zirconolite and Allanite-(Ce)* and Associated Minerals from Koberg Mine, Bergslagen, Sweden.* Mineralogical Magazine. 56, 17–35.

Received at: 04. 06. 2013
Revised at: 02. 12. 2013
Accepted for publication at: 04. 12. 2013
Published online at: 06. 12. 2013